ELSEVIER

Sensors and Actuators A 97–98 (2002) 347–358

SENSORS AND ACTUATORS A PHYSICAL

www.elsevier.com/locate/sna

A symmetric surface micromachined gyroscope with decoupled oscillation modes

Said Emre Alper, Tayfun Akin*

Department of Electrical and Electronics Engineering, Middle East Technical University, Ankara, Turkey

Received 7 July 2001; received in revised form 28 November 2001; accepted 28 November 2001

Abstract

This paper reports a new symmetric gyroscope structure that allows both matched resonant frequencies for the drive and sense vibration modes for better sensitivity, and also decoupled drive and sense oscillation modes for preventing unstable operation due to mechanical coupling and achieving a low zero-rate output drift. The symmetry and decoupling features are achieved at the same time with a new suspension beam design. The gyroscope structure is designed using a standard three-layer polysilicon surface micromachining process (MUMPS) and simulated using the MEMCAD software. The drive and sense mode resonant frequencies of the fabricated device are measured as 28,535 and 30,306 Hz, respectively, which are in agreement with the finite element simulations. The small mismatch is due to the unsymmetric distribution of the etch holes, which can be eliminated with a proper design. When the resonant frequencies are closely matched, the rate sensitivity of the gyroscope is amplified by the mechanical quality factor of the sense resonant mode. The new suspension beam structure also provides very high quality factors for the drive and sense modes, such as 10,400, when operated under 10 mTorr vacuum level. Even though the performance of the fabricated sensor is limited due to large parasitic capacitances between the mechanical structure and the substrate, measurements, and calculations show that the sensor can still sense angular rates as small as 1.6°/s under vacuum. This sensitivity can be enhanced by at least an order of magnitude if the parasitic capacitances could have effectively been eliminated. The advantage of the new structure can be combined with advanced, high-aspect ratio fabrication processes to obtain very sensitive micromachined gyroscopes.

Keywords: Symmetric gyroscope; Decoupled gyroscope; Micromachined gyroscope

1. Introduction

Micromachined gyroscopes are quite popular in many low cost applications, such as camcorder stabilization, automotive roll-over detection, and inertial mouse. However, the rate sensitivity and the drift of these devices are much worse than those of the conventional high performance ring-laser and fiberoptic gyroscopes [1], and not suitable for applications requiring inertial grade performance. There are extensive studies on increasing the performances of the micromachined gyroscopes [2–6]. One method is to implement symmetric gyroscopes with matched resonant frequencies for the drive and sense vibration modes, so that gyroscope sensitivity (resolution) is amplified with the mechanical quality factor of its sense resonance mode [1,6]. Some approaches try to match resonant frequencies by designing symmetric drive and sense suspension beams [2]. However, when the frequency mismatch between drive and sense modes is reduced, the mechanical coupling between them increases due to the nature of the suspension beams [3,4], causing unstable device operation and increased zero-rate output drift. To decrease mechanical coupling, various structures [4,5] have been proposed where the drive and sense suspension beams are independent. However, since their suspension beams are not symmetric it is not easy to match the resonant frequencies in these structures, and hence, the resonant frequencies are process dependent. Also, unsymmetrical gyroscope structures exhibits large temperature-dependence, since the stiffness of unsymmetrical suspension designs may show large shifts for the drive and sense resonant frequencies with temperature variations [7]. Therefore, this second class of gyroscopes may show a large temperature-dependent output drift.

This paper proposes a new gyroscope structure that solves the problems of mechanical coupling and mismatched resonant frequencies at the same time by using a novel symmetric suspension beam design combined with decoupled vibration modes for stable operation. Due to its symmetric

* Corresponding author. Tel.: +90-312-210-2369; fax: +90-312-210-1261.
E-mail address: tayfun-akin@metu.edu.tr (T. Akin).

0924-4247/02/$ – see front matter
PII: S0924-4247(01)00860-3

structure, its sensitivity is amplified by the mechanical quality factor of the sense mode. The gyroscope also provides a high quality factor due to its new suspension design and when operated under vacuum, and this high quality factor considerably improves the performance. Secondly, the symmetric suspension design makes the gyroscope insensitive to temperature-dependent output drift. In addition to the advantages associated with the symmetric suspension design, there are some advantages associated with the decoupled vibration modes. First of all, decoupling prevents undesired interaction between the drive and sense mode vibrations and secondly, it results in a very low zero-rate output drift. If this new structure can be implemented with high-aspect ratio processes, a very high performance gyroscope, with inertial grade rate sensitivity and drift rate, can be obtained.

2. Gyroscope structure

Fig. 1 shows the geometrical structure of the symmetric and decoupled gyroscope. The anchors of the structure are placed at the outermost corners and connected to the movable drive and sense electrodes with the help of suspension beams. This connection prevents mechanical coupling, since the oscillations of the two vibration modes do not affect each other. In addition, unlike the conventional approach, the suspension beams supporting the proof mass are not attached to the anchors directly, rather the proof mass is supported by the beams attached to the movable drive and sense electrodes, preserving the symmetry of the structure.

The gyroscope operates according to the Coriolis coupling principle. The proof mass is vibrated along y-axis by applying suitable AC excitation between the stationary and movable drive fingers and a DC polarization voltage to the proof mass. When the substrate of the gyroscope is rotated around z-axis, the proof mass tends to vibrate along x-axis due to Coriolis coupling. By measuring the amplitude of this induced vibration (sense mode), the angular rate of the applied rotation can be derived.

A common problem for vibrating gyroscopes is the cross-coupling between the drive and sense mode oscillations. The proposed structure solves this problem to a great extent due to its decoupled spring design for the two vibration modes, without destroying the symmetry of the device that is required for high rate sensitivity. The decoupled operation is verified using finite element simulation, as described in the next section.

3. Finite element simulations

Finite element simulations were used to verify the desired operation of the gyroscope. The simulations were performed with the MEMCAD 4 software package. Fig. 2 shows MEMCAD modal simulation results for the drive and sense vibration modes. Resonant frequencies of the two modes are found to be equal and 33,154 Hz ignoring the effects of the etch holes on the proof mass, internal stress of the structural polysilicon layer and the mass of the comb-fingers. When these effects are taken into account, the simulated modal frequencies are equal to 30,912 Hz, giving a more accurate estimation when compared with the measured frequencies of the fabricated devices. The matched resonant frequencies for the drive and sense vibration modes would result in an improvement in the rate sensitivity by a factor equal to the quality factor of the sense vibration mode, which can be in the order of a few thousand for polysilicon structures in vacuum. A common problem with symmetric gyroscopes is the mechanical coupling between the two vibration modes, resulting in unstable operation and drift. A major advantage of our structure is that it provides decoupled operation while having a symmetric structure.

Decoupled operation of the drive and sense modes can also be shown with finite element simulations. Fig. 3 shows the finite element simulations for the relative displacements of the two vibration modes when only one of these modes is vibrating. It is clear that during the vibration of an orthogonal mode (either drive or sense), the second orthogonal mode (sense or drive) is not affected from the vibrations in the first orthogonal mode. Numerically, the vibration amplitude of the sense electrodes is only about 2.5% of the drive mode vibration. This vibration can further be suppressed

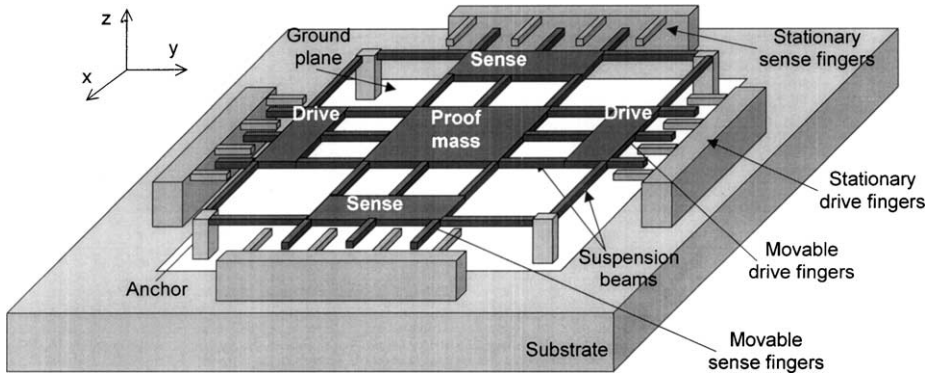

Fig. 1. Geometrical structure of the proposed symmetric and decoupled gyroscope. The mechanical coupling between the drive and sense modes is suppressed with a special placement of the anchorage and suspension beams.

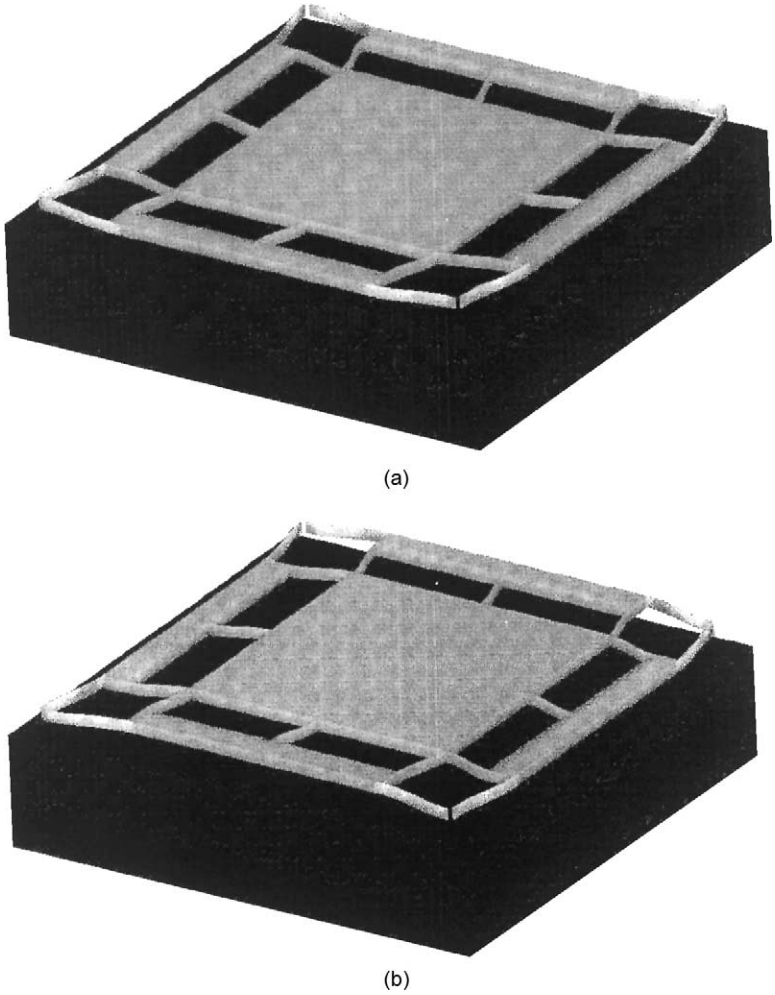

Fig. 2. MEMCAD modal simulation result for (a) the drive and (b) the sense vibration modes. Resonant frequencies of the two modes are both equal to 30,912 Hz due to the preserved symmetry. This simulation also verifies the decoupled operation of the drive and sense resonant modes.

with the differential readout scheme, since the sense electrodes operates in a differential manner. In other words, the displacements experienced by the sense electrodes are in opposite directions, therefore, the output capacitance change is equal for both sense electrodes, resulting in a zero-output after the differential readout circuit. In summary, this simulation shows that the vibration of a mode does not affect the other significantly, verifying that the mechanical decoupling between two modes is achieved with the novel structure of the suspension beams. This enhances the stability of the sensor and decreases the complexity of a feedback network.

4. Implementation and test results

The gyroscope was fabricated through a standard three-layer polysilicon surfacemicromachining process (MUMPS) provided by Cronos. Fig. 4 shows the SEM pictures of the fabricated gyroscope which measures 1 mm × 1 mm. The thickness of the structural layer is 2 μm, defined by the foundry process. Due to the thin structural layer and 2 μm allowable minimum spacing, the capacitances of the drive and sense modes are about 6.5 fF, limiting its performance. Another fact that limits the performance is the buckling that is observed in the structural polysilicon layer due to the remained residual stress after fabrication. Fig. 5 shows the SEM picture showing how large is the off-plane misalignment between the stationary and movable comb-fingers that were attached to the proof mass. This misalignment decreases the already small stationary capacitance value, resulting in less sensitivity. These limitations are related to the fabrication process of the device and the device parameters can be enhanced by advanced fabrication techniques such as high-aspect ratio micromachining technologies. Even though the MUMPS process has limited the device performance, the device still provides an acceptable sensitivity, due to the symmetric structure and very high quality factor of the gyroscope.

A number of tests were performed to verify the device operation by determining the resonant frequencies and performance. Resonant frequencies of the drive and sense

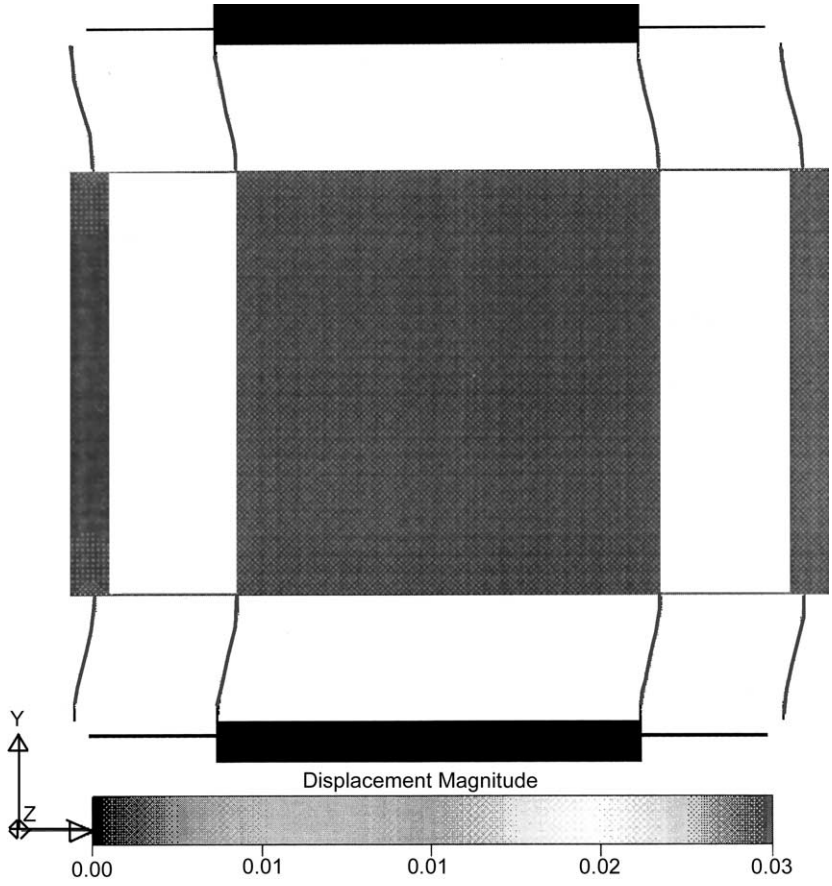

Fig. 3. Finite element simulations performed using MEMCAD showing the relative displacements of the two vibration modes when only one of these modes is excited. It is clear that the vibration of a mode does not affect the other verifying the decoupled operation of the proposed gyroscope.

vibration modes were measured by the HP4395A Network/Spectrum Analyzer. These measurements were done by using a unity-gain buffer circuit chip that was hybrid connected to the sensor. The buffer chip allows monitoring the high impedance output signal from the gyroscope. Fig. 6 shows the resonant frequency measurement results for (a) drive and (b) sense modes. The drive and sense mode resonant frequencies are measured as 28,535 and 30,306 Hz, respectively, when a 40 V DC bias (polarization) voltage is applied to the proof mass. The small mismatch between the resonant frequencies comes from the non-uniform placement of the etch holes on the proof mass due to an error in the layout and can be eliminated in the future designs. By applying different DC bias voltages separately to the drive and sense electrodes, the small mismatch between the resonant frequencies can be decreased further. Fig. 7 shows the resonant frequency shift versus DC bias voltage for the drive and sense modes. The measured frequencies are close to the simulated frequencies of 30,912 Hz when the secondary effects are also taken into account in the simulations. It should be mentioned that the above measurements were performed at atmospheric pressure and the device operation is greatly affected by the viscous air damping effect. If the measurements are performed under vacuum, the performance improves extensively, as discussed later.

The resonant frequency measurements show that the amplitudes of the resonant peaks are quite low due to parasitic degradation. Parasitic capacitance at the high impedance node of the sensor is the sum of the capacitances between the substrate and the sensor mass, interconnects, bonding pads, and the buffer input. Fig. 8 shows the parasitic capacitances and the parasitic model of the gyroscope output including the hybrid connection to the buffer chip. The parasitic capacitance at the high-impedance node of the sensor is measured using HP4294A Precision Impedance Analyzer and found to be around 5–7 pF, which is much higher than the sensor capacitances of 6–7 fF. Obviously, the output signal of the sensor is degraded by more than two orders of magnitude due to the parasitic capacitances. In fact this is verified by measuring the resonant characteristics of the gyroscope with an improved readout circuit having a smaller input capacitance and employing bootstrapping for the cancellation of parasitic capacitances. Fig. 9 shows the improvement in the resonant frequency measurement for the drive mode using this new interface circuit with bootstrapping. The new circuit reduces the parasitic capacitance at the output port of the gyroscope to less than 500 fF, resulting in

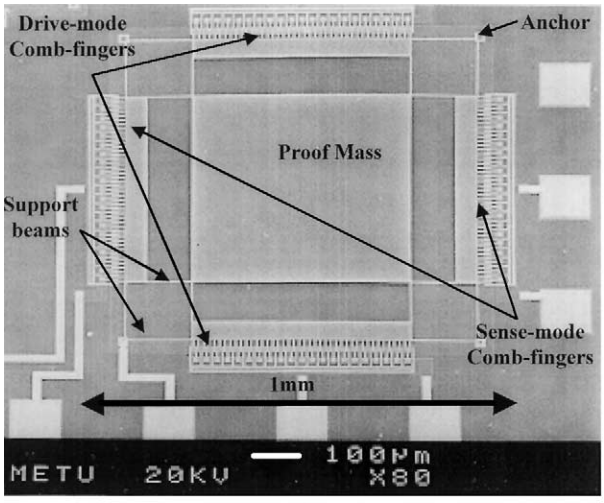

(a)

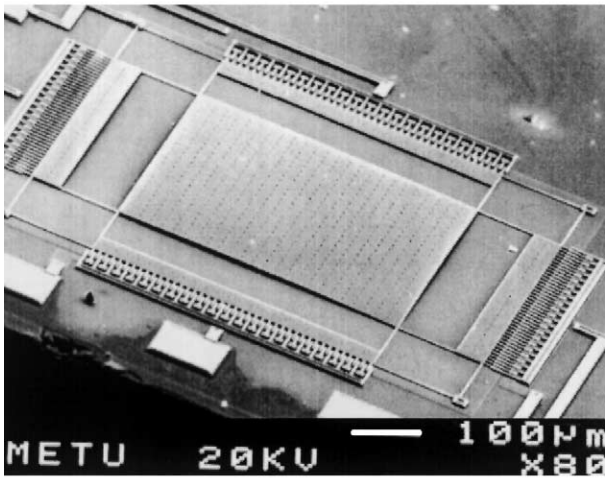

(b)

Fig. 4. SEM pictures of the fabricated gyroscope: (a) top view and (b) perspective view. The thickness of the structural layer is only 2 μm, which is limited by the MUMPS process.

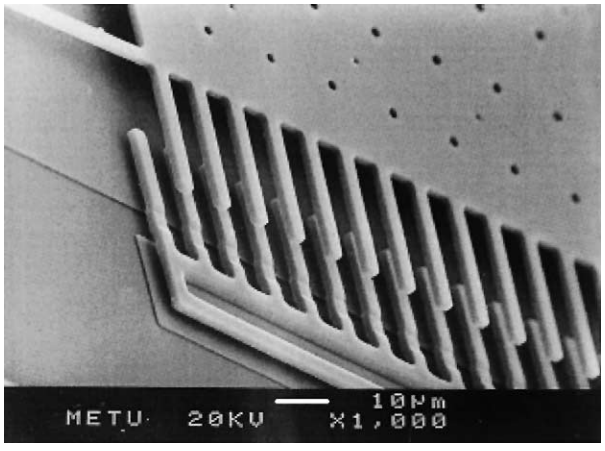

Fig. 5. SEM picture of the comb-fingers of the gyroscope, showing the buckling effects due to the internal stress of the structural polysilicon layer. The device still functions properly even with this extremely degrading effect due to its symmetric feature.

an increase at the output signal level by an order of magnitude. Further improvements can be achieved by monolithic implementation of the sensor and the readout circuits with improved bootstrapping techniques [8], which is under consideration for future symmetric and decoupled gyroscope designs.

Parasitic capacitances also cause parasitic signal coupling from the driving electrode to the sensing electrode, reducing the amplitudes of the measured resonant frequencies at atmospheric pressure. The measurement results show that the amplitudes of the resonant modes are in the order of 0.04 dB. At atmospheric pressure, the amplitude of the excitation signal is 3.56 V peak-to-peak, which is limited by the output of the used network analyzer. Such an excitation signal results in 4 μm vibration amplitude of the proof mass at resonance, which creates a 2 mV peak-to-peak signal at the gyroscope output. However, the amplitude of the noise-coupled signal at the sensing electrode is found to be about 350 mV peak-to-peak. Hence, the signal created by the gyroscope is hard to measure even at large vibration amplitudes. At this point either the driving signal amplitude should be decreased with vacuum operation or the parasitics should have been eliminated by some means such as bootstrapping methods or implementation of the structure on an insulating substrate. Unfortunately, it is not possible to eliminate the parasitic capacitances in the MUMPS process, and therefore the fabricated devices were eliminated in vacuum environment. Fig. 10 shows an illustrative simulation comparing the resonant measurements for the drive mode of the proposed gyroscope sitting over the usual conductive silicon substrate and on an insulating substrate. It was simulated that the signal coupling to the gyro output is much higher if the device is fabricated on a conductive substrate, as in the MUMPS process. These simulation results show that the limitation in the performance is due to the fabrication process used in the implementation and not due to the structure. Therefore, a much higher performance can be expected from this symmetric and decoupled gyroscope structure if it is implemented on insulating substrates.

The gyroscope measurements were also repeated under vacuum to show that its performance is greatly enhanced if the affect of air damping is reduced. Under vacuum both the drive and sense modes of the gyroscope can be excited with very small AC excitation voltages, in the order of 10 mV peak-to-peak amplitudes. With such small excitation signals, the parasitic signal coupling to the sensing electrodes are also decreases noticeably to about 1 mV peak-to-peak levels, compared to 350 mV peak-to-peak when excitation is done at atmospheric pressure. In addition, the mechanical structure demonstrates very high quality factors of above 10,000 due to the decreased effect of air damping under vacuum. Fig. 11 shows the drive mode resonance measurement at 10 mTorr vacuum, where the resonance peak appears at 28.1 kHz with a bandwidth of 2.7 Hz, giving a quality factor of 10,400. The signal-to-noise ratio at vacuum

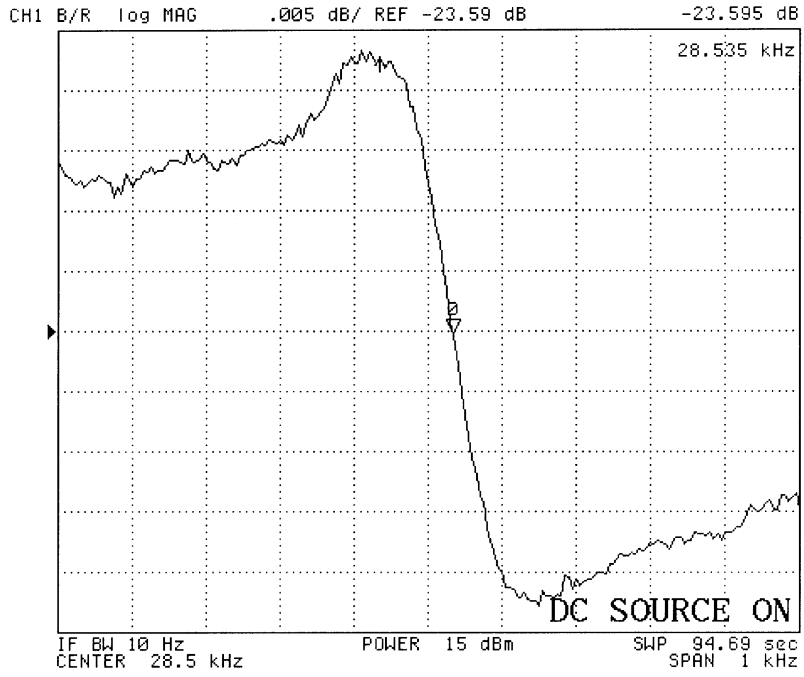

(a)

(b)

Fig. 6. Network analyzer measurement results for the resonant frequencies of the two vibration modes of the fabricated gyroscope, which are (a) 28,535 Hz for drive mode and (b) 30,306 Hz for the sense mode. The small mismatch between the resonant frequencies comes from the non-uniform placement of the etch holes on the proof mass.

also increases to 14 dB compared to the 0.04 dB at atmospheric pressure, showing significant improvement. The signal-to-noise ratio can be increased much more with some improvement in the device structure and the implementation method. These improvements can be listed as, (1) the effective elimination of the parasitic capacitances using bootstrapping methods or implementation on an insulating substrate, (2) the design of dedicated readout circuit with very high input impedance, and (3) the fabrication of the device using a thicker structural layer.

The measurement results can be used to calculate the rate sensitivity of the device with the help of analytical equations

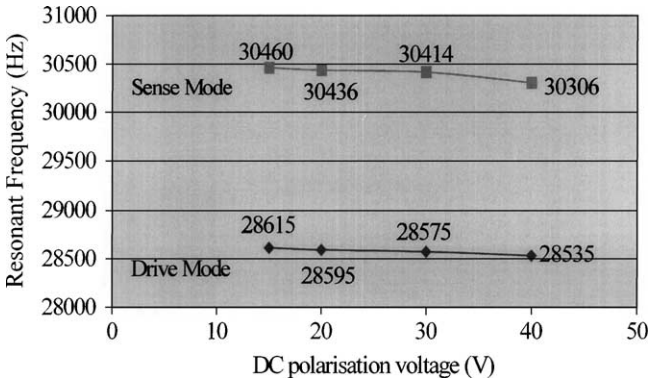

Fig. 7. Resonant frequency vs. DC bias voltage for the drive and sense modes of the fabricated gyroscope.

as explained below. The driving mode vibration can be described as,

$$x(t)_{\text{drive}} = X_0 \sin(w_x t) \tag{1}$$

where X_0 denotes the amplitude of vibration (along x-axis), and w_x the mechanical resonant frequency of the drive mode of the gyroscope. Using lumped-parameter-model for the gyroscope, the complex magnitude of the sense mode vibration as a function of the drive and sense mode resonant frequencies, applied angular rate, and the drive mode vibration amplitude can be calculated as

$$Y(\mathrm{j}w) = \frac{4\pi\Omega_0 X_0 w_x}{(w_y^2 - w_z^2) + \mathrm{j}(w_x w_y / Q_y)} \tag{2}$$

where Ω_0 is the applied rotation rate, w_y the sense mode resonant frequency, and Q_y the mechanical quality factor of the structure for the sense mode. If the drive and sense mode resonant frequencies are matched, i.e. $w_x = w_y$, then Eq. (2) simplifies to [9]

$$Y(\mathrm{j}w) = \frac{4\pi\Omega_0 X_0 Q_Y}{\mathrm{j}w_x} \tag{3}$$

meaning that the resulting sense mode displacement is amplified by the mechanical quality factor of the sense mode and lags the drive mode excitation force by 90° (factor 'j' in the denominator). This frequency matching is already satisfied in symmetric gyroscopes. For devices with unsymmetric suspensions, the frequency matching is quite difficult and requires accurate control of the spring constants in the

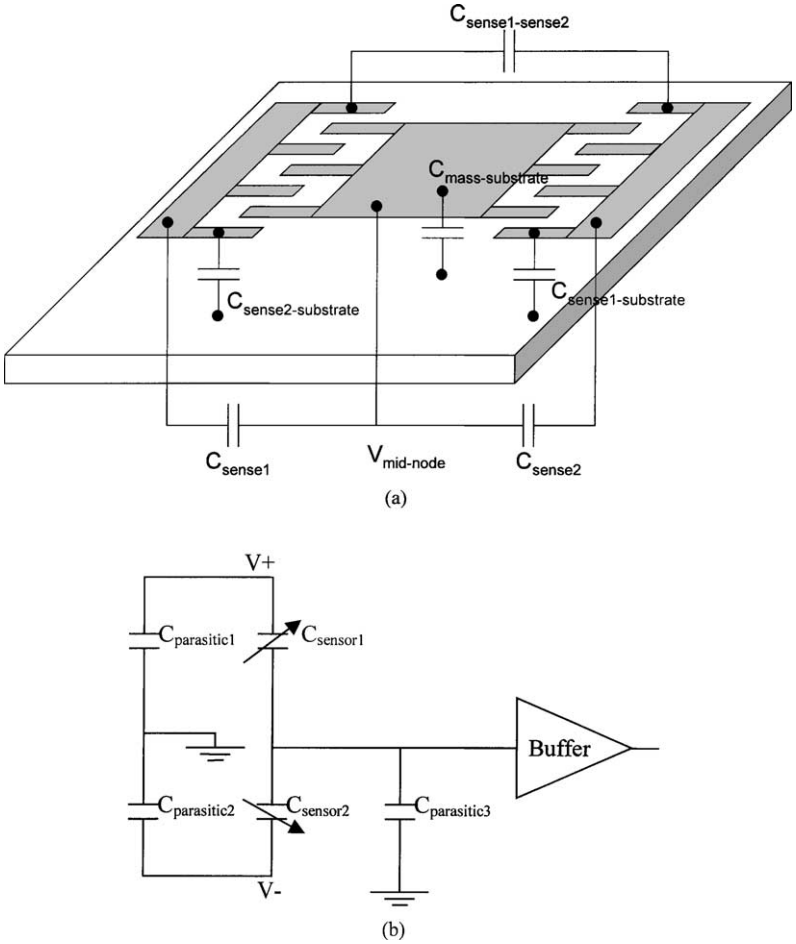

Fig. 8. (a) Parasitic capacitances and (b) the parasitic model of the gyroscope output including the hybrid connection to the buffer chip.

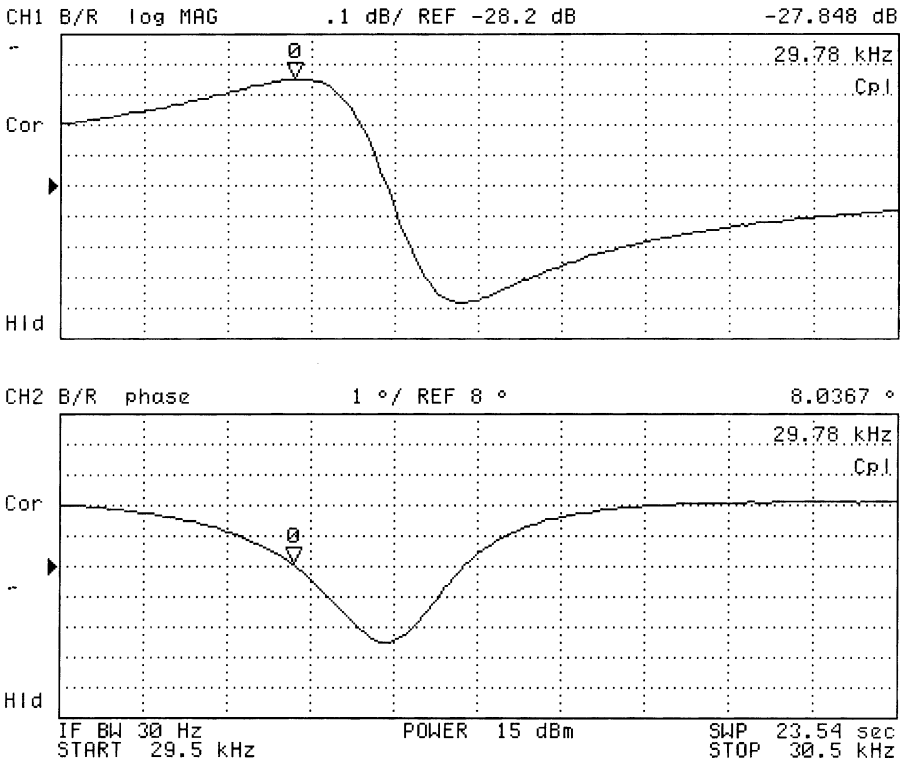

Fig. 9. The improvement in the resonant frequency measurement for the drive mode using newly designed interface circuit. The new circuit reduces the parasitic capacitance at the output port of the gyroscope to less than 500 fF, resulting in an increase at the output signal level by an order of magnitude compared to the results shown in Fig. 6.

drive and sense modes. Even the drive and sense mode frequencies of an unsymmetric gyroscope is matched with accurate design, these matching could not be conserved as the operating temperature varies. This is because the stiffness of the unsymmetric suspensions vary with different ratios resulting in a temperature-dependent performance degradation. In symmetric gyroscopes, however, the stiffness of the symmetric suspensions would vary with the same ratio, resulting in a much smaller susceptance to temperature variations. In order to illustrate how the performance of an unsymmetric gyroscope is reduced with changing temperature, Eq. (2) must be reviewed. As the temperature changes, the drive and sense mode resonant frequencies of an unsymmetric gyroscope are no more equal to each other, i.e. $w_x \neq w_y$. Furthermore if the device is operated at vacuum with a high Q_y, which is the usual case, then the imaginary part of the denominator of Eq. (2) would be negligible compared to the $(w_y^2 - w_x^2)$ term. Then the sense mode vibration should be recalculated as

$$Y(\mathrm{j}w) = \frac{4\pi\Omega_0 X_0 w_x}{w_y^2 - w_x^2} \tag{4}$$

Clearly, the output response of the gyroscope is reduced by a factor of approximately 0.5 $Q_y/(w_y - w_x)$ and is in-phase with the drive mode excitation voltage. Therefore not only the sensitivity decreases by changing temperature, but also the output of the gyro would be susceptible to in-phase parasitic signal coupling from the input of the gyroscope. This analysis clarifies the advantage of using symmetric suspensions with matched resonant frequencies. Switching back to the matched resonant frequencies case of Eq. (3), the rate sensitivity of the symmetric gyroscope can be calculated. For the excitation conditions used in the measurements shown in Fig. 11, the drive mode vibration amplitude was optically determined as 4 μm. For performance estimation, we can assume the drive and sense vibration modes are matched at 30 kHz. Using this resonant frequency value and the measured quality factor of 10,400 in Eq. (3), the peak vibration amplitude of the sense mode of the gyroscope is found to be around 80 Å for a 1°/s external rotation rate. This vibration amplitude results in a 11.9 aF capacitance change, and the device has a 0.9 mV/(°/s) scale factor. For the fabricated devices, the parasitic capacitances, and hence, the direct parasitic signal coupling from the input to the output node is quite high, in the order of 1 mV. Therefore, the rate sensitivity of the device is currently 1.6°/s. However, this sensitivity value can be enhanced to better than 0.16°/s if the parasitic signal coupling can be kept below −40 dB, which is possible if parasitic capacitances can be effectively eliminated by implementing the structure on an insulating substrate. These calculations show that the implementation of this new structure on an insulating substrate with advanced and high-aspect ratio fabrication techniques will allow obtaining a very high sensitivity gyroscope.

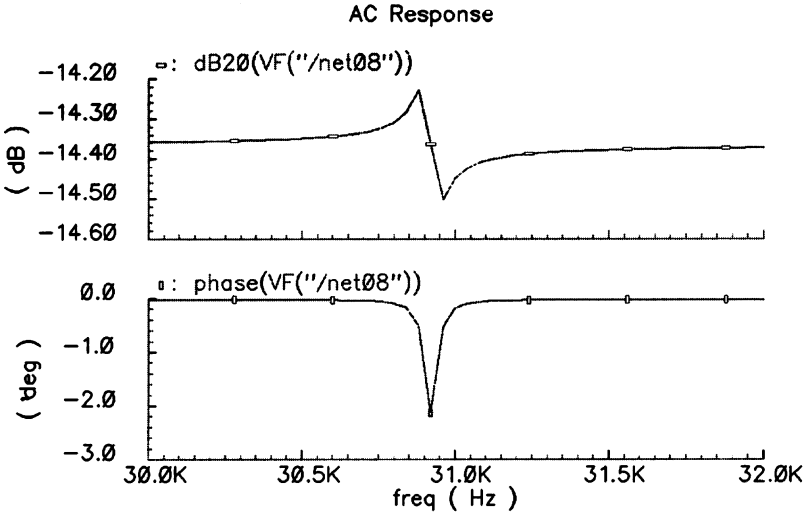

(a)

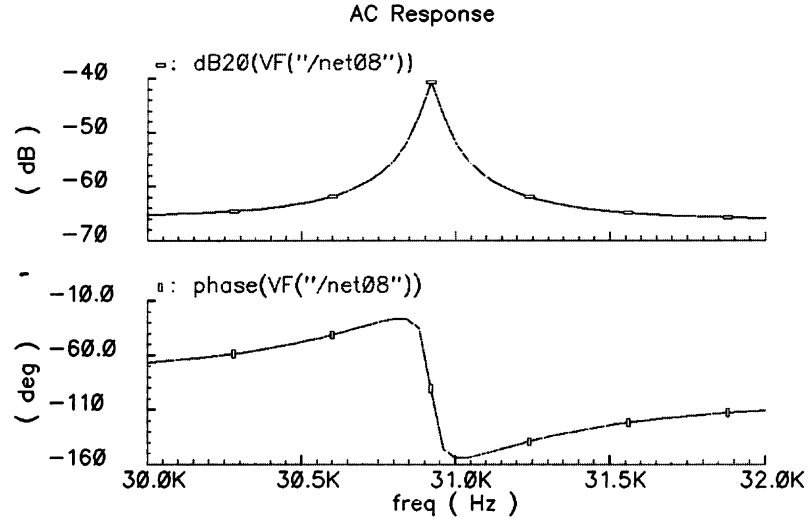

(b)

Fig. 10. An illustrative simulation comparing the resonant measurements for the drive mode of the proposed gyroscope sitting over (a) the usual conductive silicon substrate and (b) an insulating substrate. It is obvious that, the signal-to-noise ratio in (b) is much greater than that in (a) because of reduced parasitic signal coupling through the substrate.

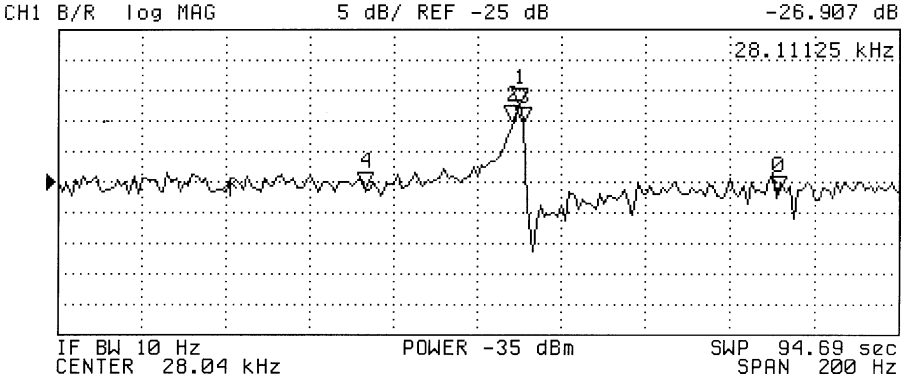

Fig. 11. The drive mode resonance measurement at 10 mTorr vacuum, where the resonance peak appears at 28.1 kHz with a bandwidth of 2.7 Hz, giving a quality factor of 10,400. Here note that the peak is clearly visible even though there is excessive parasitic coupling to the output from the input excitation signal.

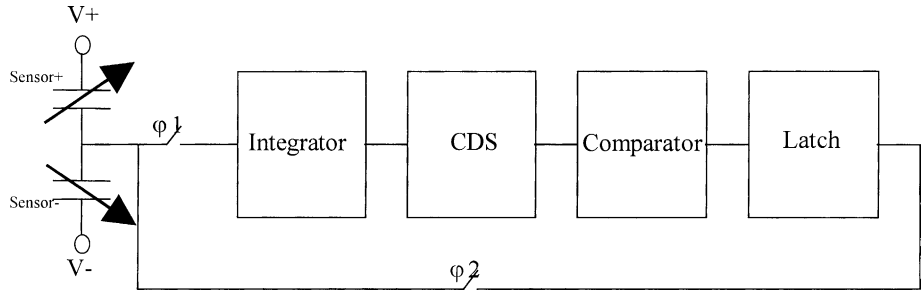

Fig. 12. Block diagram of the capacitive readout circuit. Non-overlapping clocks φ_1 and φ_2 are for processing and for feedback, respectively.

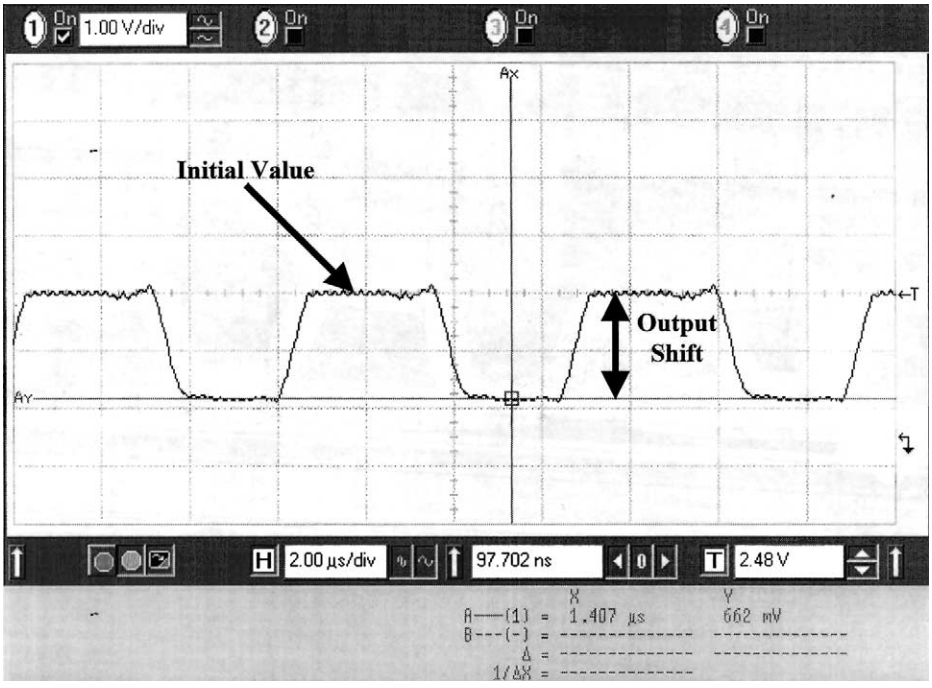

Fig. 13. The output of the readout circuit when there is 40 fF mismatch between the capacitors forming the half-bridge in Fig. 12. The output voltage shift is 1.8 V, corresponding to a sensitivity of 45 mV/fF and can detect capacitance changes smaller than 0.1 fF.

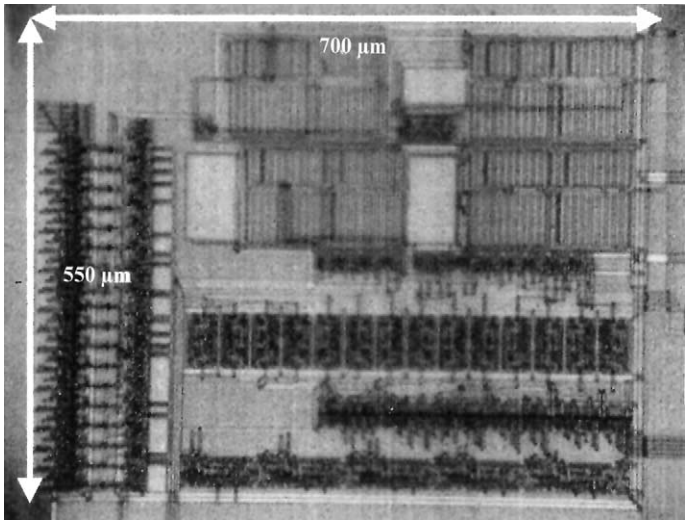

Fig. 14. Photograph of the fabricated readout circuit. The readout circuit was designed in 0.8 µm CMOS process of AMS. It can detect capacitances smaller than 0.1 fF with sensitivity close to 45mV/fF.

5. Readout electronics

A capacitive readout circuit was also designed and fabricated in a standard 0.8 μm CMOS process to be used with the fabricated device. Fig. 12 shows the block diagram of the proposed readout circuit that uses the charge amplification method. The circuit senses the difference between the capacitors $C_{\text{sense}+}$ and $C_{\text{sense}-}$ and shifts the voltage at the common node of the capacitors. This shift is integrated by the integrator, which is then fed to the correlated double sampling (CDS) circuit. The CDS block is used for canceling possible shifts, which may arise due to op amp offsets and switch noises. The CDS output is connected to the comparator, whose output is a 1 bit digital signal. For closed loop operation this signal may be processed by a latch, and the latch output can be fed back to the common node of the capacitors canceling the sensor capacitance deflection.

The readout circuit is tested and verified to detect capacitance changes smaller than 0.1 fF, with a sensitivity of 45 mV/fF. Fig. 13 shows the output of the readout circuit when $C_{\text{sensor}+}$ is 40 fF larger than $C_{\text{sensor}-}$. Then, the output voltage shifts about 1.8 V, showing that the circuit provides a sensitivity of 45 mV/fF and detects capacitance changes smaller than 0.1 fF. Fig. 14 shows the photograph of the fabricated readout circuit. When hybrid connected to the gyroscope chip, the readout circuit operation is degraded due to high parasitic capacitances associated with the gyroscope. Hence, a new readout circuit is designed and fabricated, which uses bootstrapping method to cancel the parasitic capacitances.

6. Conclusions and future work

A new symmetric gyroscope structure is presented that allows not only matched resonant frequencies for the drive and sense vibration modes for better resolution and low temperature-dependent drift, but also decoupled drive and sense oscillation modes for preventing unstable operation and zero-rate output drift due to mechanical coupling. The device operation is verified by FEM simulations using MEMCAD software, and the resonant frequencies of the drive and sense vibration modes are measured to be close to the simulated results. It was shown that operation is highly improved at vacuum environment. Recent measurements under 10 mTorr vacuum condition and calculations show that the structure can provide a rate sensitivity better than 1.6°/s with a 0.9 mV/(°/s) scale factor if the drive and sense mode resonant frequencies of the device could be closely matched, which can be improved further to 0.16°/s by eliminating the parasitic capacitances. This performance is currently limited with the available fabrication process where the structural layer thickness is about 2 μm. But the new structure can be implemented with advanced micromachining processes that have thicker structural layers fabricated on insulating substrates to obtain high-performance gyroscopes. A capacitive readout circuit has also been designed and fabricated in a 0.8 μm CMOS process, and it can detect capacitance changes smaller than 0.1 fF with a sensitivity of 45 mV/fF, providing enough sensitivity for the fabricated symmetric gyroscopes.

Acknowledgements

This work is sponsored by the National Defense Ministry and The Scientific and Technical Research Council of Turkey (TUBITAK).

References

[1] N. Yazdi, F. Ayazi, K. Najafi, Micromachined inertial sensors, Proc. IEEE 86–88 (1998) 1640–1659.
[2] S.S. Baek, Y.S. Oh, B.J. Ha, S.D. An, B.H. An, H. Song, C.M. Song, A symmetrical *z*-axis gyroscope with a high aspect ratio using simple and new process, in: Proceedings of the IEEE Micro Electro Mechanical Systems Workshop, 1999, pp. 612–617.
[3] H. Kawai, M. Tamura, K. Ohwada, Direct measurement of mechanical coupling in microgyroscope using a two-dimensional laser displacement meter, in: Proceedings of the 10th International Technical Digest Conference on Solid-State Sensors and Actuators, 1999, pp. 1566–1569.
[4] Y. Mochida, M. Tamura, K. Ohwada, A micromachined vibrating rate gyroscope with independent beams for the drive and detection modes, in: Proceedings of the IEEE Micro Electro Mechanical Systems Workshop, 1999, pp. 618–623.
[5] W. Geiger, J. Merz, T. Fischer, B. Folkmer, H. Sandmaier, W. Lang, The silicon angular rate sensor system MARS-RR, in: Proceedings of the 10th International Technical Digest Conference on Solid-State Sensors and Actuators, 1999, pp. 1578–1581.
[6] F. Ayazi, K. Najafi, Design and fabrication of a high-performance polysilicon vibrating ring gyroscope, in: Proceedings of the IEEE Micro Electro Mechanical Systems Workshop, 1998, pp. 621–626.
[7] F. Ayazi, A high-aspect ratio high-performance polysilicon vibrating ring gyroscope, Ph.D. Dissertation, The University of Michigan, 2000.
[8] C. Lu, M. Lemkin, B.E. Boser, A monolithic surface micromachined accelerometer with digital output, IEEE J. Solid-State Circuits 30–32 (1995) 1367–1373.
[9] W.A. Clark, R.T. Howe, Surface micromachined *z*-axis vibratory rate gyroscope, in: Proceedings of the Technical Digest Conference on Solid-State Sensor and Actuator Workshop, 1996, pp. 283–287.

Biographies

Said Emre Alper was born in Ankara, Turkey, in 1976. He received the BS and MSc degrees from the Middle East Technical University (METU) in Ankara, both in Electrical and Electronics Engineering in 1998 and 2000, respectively. Since 1998, he has been working as a Research Assistant at METU in the Department of Electrical and Electronics Engineering MEMS-VLSI Research Group. His research interests include capacitive inertial sensors, micromachined resonators and actuators, and capacitive sensor interfaces. Together with Prof. Tayfun Akin, he won the first prize award in the operational designs category of the international design contest organized by DATE and CMP in March 2001, for his symmetric and decoupled gyroscope design.

Tayfun Akin was born in Van, Turkey, in 1966. He received the BS degree in Electrical Engineering with high honors from Middle East Technical University, Ankara, in 1987 and went to the USA in 1987 for his graduate studies with a graduate fellowship provided by NATO Science Scholarship Program through the Scientific and Technical Research Council of Turkey (TUBITAK). He received the MS degree in 1989 and the PhD degree in 1994 in electrical engineering, both from the University of Michigan, Ann Arbor. Since 1995 and 1998, he has been employed as an Assistant Professor and Associate Professor, respectively, in the Department of Electrical and Electronics Engineering at Middle East Technical University, Ankara, Turkey. He is also the technical coordinator of METU-MET, an IC fabrication factory which is transferred to Middle East Technical University by the government for micro-electro-mechanical systems (MEMS) related production. His research interests include MEMS, infrared detectors and readout circuits, silicon-based integrated sensors and transducers, and analog and digital integrated circuit design. He is the winner of the First Prize in Experienced Analog/Digital Mixed-Signal Design Category at the 1994 Student VLSI Circuit Design Contest organized and sponsored by Mentor Graphics, Texas Instruments, Hewlett-Packard, Sun Microsystems, and Electronic Design Magazine. He is the co-author of the symmetric and decoupled gyroscope project which won the first prize award in the operational designs category of the international design contest organized by DATE Conference and CMP in March 2001.